Thermochimica Acta 512 (2011) 247–253

Contents lists available at ScienceDirect

Thermochimica Acta

journal homepage: www.elsevier.com/locate/tca

Characterization of surface plasmon energy transduction in gold nanoparticle/polymer composites by photo-DSC

B. Nearingburg, A.L. Elias*

Department of Chemical and Materials Engineering, University of Alberta, ECERF, Edmonton, Alberta, Canada T6G 2V4

ARTICLE INFO

Article history:
Received 22 July 2010
Received in revised form 26 October 2010
Accepted 2 November 2010
Available online 11 November 2010

Keywords:
Photo-DSC
Gold nanoparticles
Surface plasmon resonance
Stimulus-responsive polymers
Composites
Laser

ABSTRACT

In this study, we investigate the formulation and optimization of stimulus-responsive composites consisting of gold nanoparticles in polyethylene glycol diacrylate (PEGDA) matrices, which can be remotely heated through localized surface plasmon resonance (SPR). In these materials, laser radiation is absorbed by the nanoparticles and transduced into thermal energy. Optothermal properties of the polymer/nanoparticle composites are characterized using an adaptation of photo-differential scanning calorimetry (photo-DSC), in which a sample is characterized in isothermal mode in the presence and absence of optical illumination. Au/PEGDA composite samples are determined by photo-DSC to transduce energy from a 532 nm optical source with high efficiencies (>80%). UV/Vis/NIR spectrophotometry is used to characterize the optical properties of the samples. Nanoparticle dispersion and size within composite polymer matrices are characterized using transmission electron microscopy (TEM). It is shown that the magnitude and rate of energy transduction can be tuned by varying both nanoparticle concentration and dispersion.

1. Introduction

Stimulus responsive polymers are a class of materials which undergo property changes when exposed to appropriate external stimuli. For example, materials have been developed which change their physical dimensions due to variations in temperature [1], pH [2], or optical illumination [3], as have materials which alter their surface chemistry or hydrophilicity upon exposure to specific chemical compounds [4] or external electromagnetic fields [5].

Materials which can be actuated by exposure to a remote stimulation (i.e., without physical contact) are of interest for a variety of applications, including drug delivery systems and implanted biomedical devices, which by their very nature require a triggering stimulus applied external to the body [1,6–9]. Several microfluidic devices have shown improved portability, functionality, and simplicity when off-chip rather than on-chip stimuli are used to drive active components [10,11]. One method of engineering stimulus-responsive materials is to form composites consisting of a polymer matrix embedded with stimulus-active nanoparticles. The particles act as nanoscaled transducers, coupling energy from the external source into heat via loss mechanisms specific to the particular nanoparticles. This heat is transferred to the polymer, causing a temperature-driven change in its properties or dimensions. A number of stimulus-responsive polymers have been engineered in which magnetic nanoparticles absorb electromagnetic energy, which is supplied by an inductive heater [1,12–14].

Like magnetic nanoparticles, noble metal nanoparticles (including gold nanoparticles) strongly couple energy from an external stimulus, in this case via surface plasmon resonance [15–18]. Energy from incident photons creates electronic oscillations over the surface interface. Most of this energy is gradually converted into heat due to resistive losses, and this heat is then released from the surface and travels through the bulk of the material, or into the surrounding system [19]. Gold nanoparticles are well suited for use in optical heating, as only a minute fraction ($\sim 10^{-6}$) of light absorbed by the particles will be re-emitted due to effects such as photoluminescence, while the majority is converted into heat [20]. This transducing effect has been exploited for use in cancer treatment: Au nanoparticles are functionalized with ligands that bind preferentially to cancerous cells; the cancer-bound particles are then selectively heated using a laser, causing localized heating of the cells and selective necrosis [21–24]. Surface plasmon resonance is an effective means to trigger these light-based responses and controllably couple energy from incoming light into a material. The range of absorbed wavelengths may be tuned by varying the size, geometry, and composition of the nanoparticles; additionally, the strength of the absorption can be engineered through variations in particle concentration [25–28]. For example, colloidal solutions of spherical 10 nm gold nanoparticles appear red since these particles absorb light in the green portion of the spectrum,

* Corresponding author. Tel.: +1 780 248 1589; fax: +1 780 492 2881.
E-mail address: aelias@ualberta.ca (A.L. Elias).

0040-6031/$ – see front matter © 2010 Elsevier B.V. All rights reserved.
doi:10.1016/j.tca.2010.11.005

while solutions of similarly sized gold nanorods are blue-shifted to a degree determined by both the particle aspect ratio and size [29]. A beneficial use of this property involves *in vivo* biomedical applications, as nanoparticle dimensions can be chosen such that an excitation wavelength can pass through tissue but still be strongly absorbed by nanoparticles [30].

Before optically excited nanoparticles can be employed in stimulus-responsive polymers, factors affecting heating in these systems must be understood, and several investigations have been previously undertaken. In an attempt to measure the minute heat flow expected from individual particles, Richardson et al. [31] embedded gold nanoparticles in ice and irradiated the particles with a laser (with intensity of up to 1.5×10^4 W/cm^2). The volume of ice melted around each particle (or cluster) was then used to calculate the energy transduced by individual particles or small aggregations of particles. Theoretical derivations of the short time scale (picoseconds) kinetics of particle heating (in the context of selective nanolithographic patterning) were developed by Cortie et al. [32]. Their work involved a layer of polymeric resist beneath a thin layer of gold colloid solution; the resist became thermally crosslinked due to heating in the local area immediately surrounding each nanoparticle. It was found that particles with diameters of 40–50 nm could be used to locally heat the resist to between 120 °C and 160 °C, using a 521 nm laser with an irradiance of 7.19×10^4 W/cm^2. In each of the aforementioned studies, the focus was on localized rather than bulk heating effects. Characterization of bulk systems has also been undertaken. In an attempt to deduce the efficiency of energy transduction in a solution of aqueous Au nanoparticles, Roper et al. [33] irradiated a small glass cell filled with solution with a laser of incident power between 1.2 and 2.4 W/cm^2, while monitoring the temperature of the system with a thermocouple in contact with the solution. In this configuration, surprisingly low energy transduction efficiency, ~0.1, was observed. Richardson et al. [34] also measured energy transduction in an aqueous solution of Au nanoparticles, in this case by embedding a thermocouple directly within a single drop of solution suspended from a capillary. In these experiments, energy transduction efficiencies near 1.0 (for irradiation of 200–400 W/cm^2) were measured, suggesting that near lossless transfer of energy is possible.

The purpose of our work is to characterize and optimize energy transduction in stimulus-responsive polymer/gold nanoparticle composites upon exposure to a narrow band optical source. When attempting to characterize heating effects in these and other composites by measuring temperature changes, heat transfer between the composite and its surroundings must be carefully taken into account. In our investigation, we use a custom-built laser photo-differential calorimetry (photo-DSC) set-up to directly measure bulk heat flow in polymer/gold nanoparticle composites. In conventional DSC, a well-insulated sample is placed in good thermal contact with a detector, ensuring that the heat flowing out of the sample is transmitted to the detector and measured. Due to the high thermal conductivity of the pans and conducting block, virtually all of the heat produced by the samples can be recorded by the device and compared to a blank reference pan yielding accurate measurements of heat flux (on the order of μW). This instrument is expected to provide a much more precise method of thermal measurement than other indirect techniques. Photo-DSC is an adaptation of DSC wherein changes in thermal properties are measured upon exposure to light. Traditionally, photo-DSC has been used to investigate kinetics of processes such as photo-curing of polymers [35–37]. In our study, this sensitive technique will be used to precisely quantify the amount of heat generated in polymer/gold nanoparticle composites under laser irradiation and to understand how the characteristics of these composites (such as particle concentration and dispersion) affect their heating behavior.

2. Experimental

2.1. Materials

In our work, gold nanoparticles were obtained as an aqueous 10 nm citrate capped gold colloid solution (#G1527, Sigma–Aldrich) with a concentration of 0.005% (w/v). Composites were formed using poly(ethylene-glycol) diacrylate as a matrix material (#455008, Sigma–Aldrich) which was crosslinked using 2,2-dimethoxy-2-phenylacetophenone (#196118, Sigma–Aldrich) photoinitiator. All materials were used as received unless otherwise noted.

2.2. Sample preparation

To form PEGDA/Au composites with different concentrations, nanoparticles from the colloid solution were isolated and added to a PEGDA monomer/initiator mixture which was subsequently photopolymerized. Nanoparticles were typically concentrated by centrifugation at 12,000 rpm for a period of 30 or 60 min in an Eppendorf 5415D centrifuge. After centrifugation, the supernatant was extracted with a pipette. The separated supernatant was colorless, suggesting that the majority of the nanoparticles were isolated in the precipitate. The concentrated particles were re-suspended in liquid PEGDA monomer, to which approximately 0.05 wt% of 2,2-dimethoxy-2-phenylacetophenone was added. PEGDA/Au/crosslinker solutions were thoroughly blended in a vortex mixer for 5 min and subsequently sonicated for 5 min to ensure uniform dispersion of particles throughout the solutions. The solutions were then polymerized under UV irradiation at 365 nm from an 8 W source for 5 min and annealed at 65 °C on a hotplate overnight to ensure full curing of the polymer and removal of any residual water in the composite matrix. The thermal stability of both dried Au nanoparticles and polymer/nanoparticle composites was investigated by TGA. No decomposition events were observed at temperatures used in the sample preparation process. Each sample was prepared in PDMS molds using 25 μL of solution to form discs of polymer/nanoparticle composite with an average radius of 3.0 mm, average thickness of 0.7 mm, and average mass of 22 mg.

2.3. Photo-differential calorimetry

A photo-differential calorimetry (photo-DSC) apparatus was constructed through modification of a TA Q1000 DSC with a custom fitted quartz plate and an insulating polystyrene lid. A circular hole of 1 cm diameter was drilled through the insulating layer, allowing an external laser source to directly illuminate the sample pan while maintaining thermal insulation. Samples were exposed to repeating off/on illumination cycles, and the amount of heat coupled to each sample was measured as an output heat flux recorded by the DSC. Temperature and magnitude of heat flux were calibrated using an indium metal standard.

The optical source was a 4.1 mW laser operating at 532 nm. The laser spot diameter was 2.4 mm at the operating distance (14.5 cm) leading to a measured irradiance of 108 mW/cm^2. Approximately 65% of the surface area of each sample was illuminated by the laser during characterization. The actual intensity of the beam at the sample will be reduced due to reflections at each surface of the quartz plate, as well as the surface of the sample itself. Typically, a reflection of 4% can be expected at each air–glass interface, and this loss was confirmed here by measuring the transmission of a beam through a quartz plate by spectrophotometry. Since the refractive indices of quartz and polymer are similar, the polymer–air interface was assumed to have the same properties as measured for the quartz–air interface. Consequently, the intensity of the beam at the surface is 95 mW/cm^2, and the overall intensity of the light inci-

dent on the sample is 3.6 mW. Periodic measurements of the laser intensity were undertaken to ensure consistent output energy. All samples were characterized five times (on different days) and the recorded heat flux readings averaged to lessen the impact of effects such as ambient environmental variations (temperature, humidity or other effects). Crosslinked composite samples were measured in open-top aluminum DSC pans. 50 mL/min of nitrogen purge gas was passed through the DSC during all measurements.

2.4. Spectrophotometry

To determine the optical absorbance spectra of the composites and colloid solutions, a Perkin-Elmer Lambda 900 UV/Vis/NIR spectrophotometer was used in transmission mode. All spectra were recorded over the range from 400 to 700 nm, with an optical resolution of 1 nm. Liquid samples were placed in 1 cm polystyrene cuvettes, while solidified samples were directly mounted in the beam-path.

2.5. Transmission electron microscopy

TEM analysis was used to measure possible changes in particle size or clustering after nanoparticles were embedded in a crosslinked composite. Through TEM, qualitative measures of dispersion can be directly obtained. Both solidified samples and nanoparticles cast from liquid suspensions were imaged on carbon coated grids. Solidified samples were prepared using microtomed sections, while matrix-free particles were prepared through drop casting from fluidic suspensions.

3. Results and discussion

3.1. Measurement of energy transduction

3.1.1. Composite properties

Au nanoparticle/polymer composites were prepared by photopolymerizing a mixture of nanoparticles, PEGDA monomer, and photoinitiator in a PDMS mold with dimensions similar to a standard DSC pan. This shape ensured that good thermal contact was made between the sample and pan during characterization. The concentration of the samples ranged from 0.016 to 1.12×10^{-6} g_{Au}/g_{PEGDA}; samples with a range of concentrations are shown in Fig. 1a. To confirm that the nanoparticles were well-dispersed within the polymer matrix, TEM analysis was employed on both the gold colloid solution and a selection of composite samples. Typical images are shown in Fig. 1c and d. Agglomerations of particles were not seen by TEM, and as such we are confident that the particles are well-dispersed throughout the bulk of the composite materials.

The optical properties of the composite materials were characterized using spectrophotometry. We found that both the colloidal suspensions of Au nanoparticles and the composites demonstrated large absorbance maxima centered around 530 nm, as shown in Fig. 2. The slight broadening of the absorbance maximum in the polymer matrix relative to the colloid solution suggests that there are interactions between the nanoparticles and surrounding polymer which affects the SPR properties of the Au particles (*vide infra*). Based upon these optical characteristics, a green laser operating near the absorbance maximum at 532 nm was selected to provide illumination for these experiments; the measured laser source output power was 4.1 mW distributed over a spot size of 2.4 mm at operating conditions.

3.1.2. Photo-DSC characterization

Measurements of energy transduction were undertaken using a differential photocalorimetry apparatus (schematically shown in Fig. 1e). To directly and quantitatively measure the energy transduced by the composite materials, the photo-DSC apparatus was operated in isothermal mode. The instrument was set to maintain a constant temperature of 20 °C. The laser beam could then be switched on and off, causing a shift in the equilibrium heat flux. When the laser was switched on, energy was coupled from the beam to the sample, causing heating of the polymer matrix. An exothermic flux was therefore required to maintain a constant temperature within the sample. After a certain amount of time, an equilibrium state would be reached between the heat being produced by SPR and the heat flowing out of the sample. In this

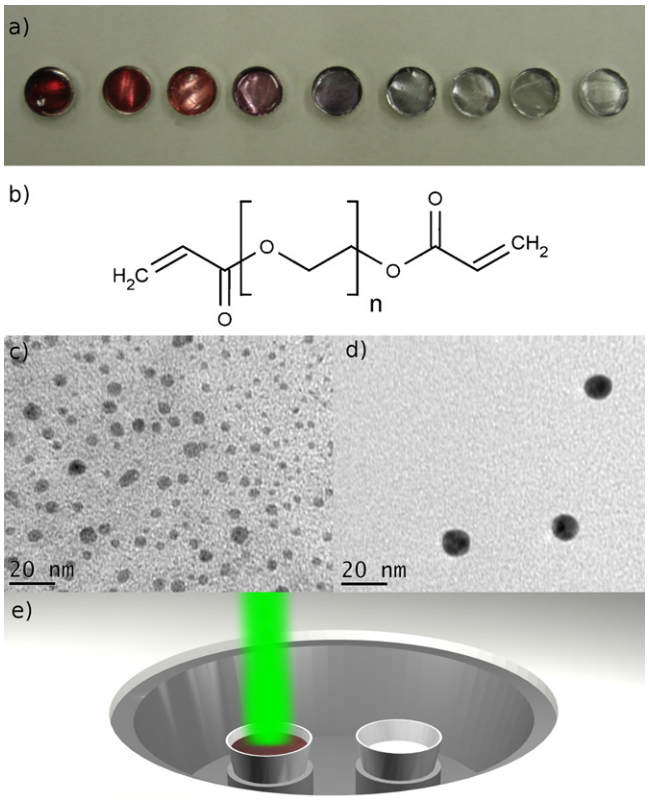

Fig. 1. (a) Cured Au/PEGDA composites in aluminum DSC pans of decreasing concentration from 8.9×10^{-7} to 1.6×10^{-8} g_{Au}/g_{PEGDA}, (b) schematic diagram of uncrosslinked PEGDA, TEM images of (c) microtomed Au/PEGDA and (d) drop cast Au colloid solution, and (e) a schematic diagram of the photo-DSC apparatus with laser illumination.

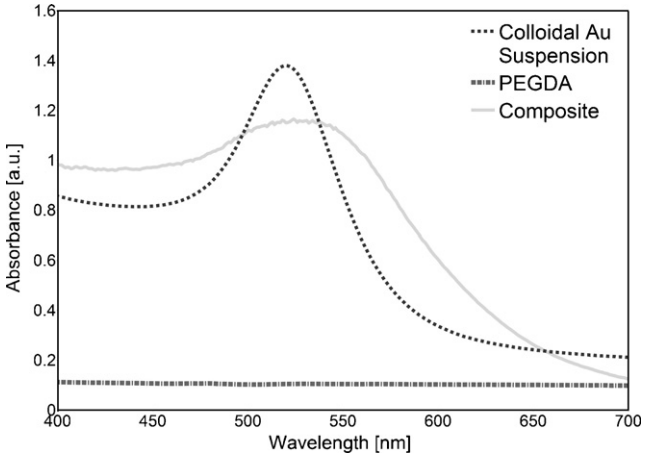

Fig. 2. UV–Vis absorbance spectra of pure PEGDA, colloidal gold solution, as well as a crosslinked Au/PEGDA composite measured by spectrophotometry.

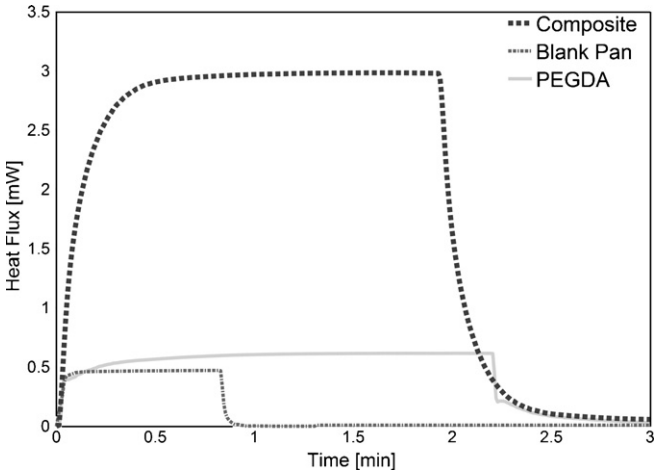

Fig. 3. Photo-DSC heat flux measurements of a blank DSC pan, pure PEGDA, and Au/PEGDA composite of 5.1×10^{-7} [g_{Au}/g_{PEGDA}] concentration. At time $t = 0$ laser light is applied to the surface of the sample which continues until a steady state is reached. For each sample, the abrupt reduction in heat flux corresponds to the removal of the laser light.

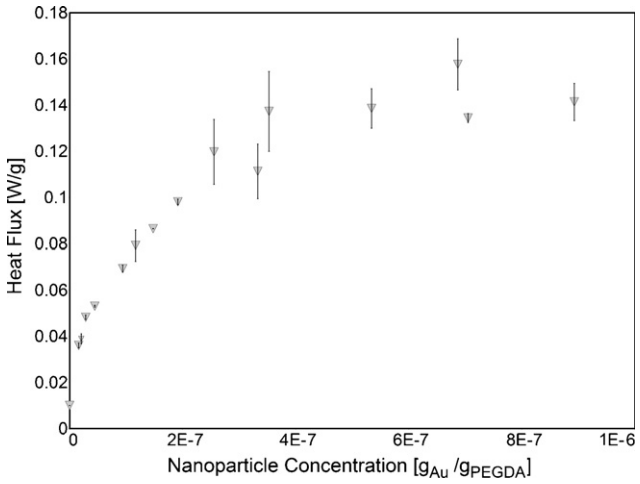

Fig. 4. Steady state heat flux as a function of concentration for Au/PEGDA composites.

state, the rates of energy influx and outflux are balanced, and hence the amount of energy transduced from the laser source into the composite was equal to measured heat flux. For a typical sample, constant heat flux readings (which fluctuated by <0.001 mW/s) were achieved within 2–3 min. Upon removal of the laser source, the samples returned to their previous equilibrium heat flux values. An example of characteristic photo-DSC heating curves for an Au/polymer nanocomposite, pure polymer, and empty pan baseline sample are given in Fig. 3. All three curves in Fig. 3 show near instantaneous changes in heat flux when the laser is turned on or off. The fast response of the blank pan is likely due to the high thermal conductivity of the aluminum itself, whereas the thermal response of the polymer samples is delayed slightly as heat is conducted through the sample.

The magnitude of energy coupling between differing equilibrium states is easily apparent from comparing the initial and irradiated exothermic heat flux measurements in Fig. 3. Measured heating curves displayed similar shape and time dependence to those presented in Richardson et al. [34], where temperature rather than heat flux was plotted as a function of time. Optimization of the photo-DSC characterization method required additional baseline correction to be certain that the measured effects were due to SPR energy transduction within the polymer samples alone and not other anomalous effects (such as heat gained or lost from the environment). When the isothermal equilibrium heat flux flowing from a blank pan was measured, it was found that 0.47 ± 0.05 mW of energy was coupled from interactions with the pan alone (measured by exposing a blank pan to the laser source and recording the difference in heat flux, as is shown in the lower curve in Fig. 3). For samples with decreasing concentrations of nanoparticles, this factor becomes an increasingly dominant portion of the overall heating, as is shown in the PEGDA curve in Fig. 3. For the purposes of analysis, this equilibrium baseline was subtracted from the measured heat flux for all samples. The baseline isothermal heat flux for pure PEGDA was also measured, and was found to be 0.012 ± 0.004 W/g. Pure PEGDA likely couples energy from the optical source through the presence of residual photoinitiator which remains in the samples after the crosslinking process and is known to absorb a wide range of visible radiation [38].

The steady-state heat transduced by the composite materials as measured by photo-DSC was plotted as a function a particle concentration in Fig. 4. At the lowest concentrations (0.1×10^{-7} to g_{Au}/g_{PEGDA}), the amount of energy transduced is similar to the amount of energy coupled by pure PEGDA. As the concentration of nanoparticles in the composite increases, a commensurate linear increase in energy transduction is seen. At higher nanoparticle concentrations (>3×10^{-7} g_{Au}/g_{PEGDA}), the magnitude of energy transduction converges to near 0.14 ± 0.01 W/g, largely independent of concentration. These results can be explained by considering the magnitude of light passing through the samples. At low nanoparticle concentrations, only a small portion of the incident light is coupled into the system, while a large portion passes through unabsorbed. As nanoparticle concentration increases, absorbance increases until all of the light is absorbed. Further increasing the concentration of nanoparticles beyond this threshold does not lead to enhanced heat flux, since all of the energy from the laser is already absorbed (neglecting losses to air, scattering, etc.). This hypothesis is supported by the measured spectrophotometer absorbance curves of the composites characterized by photo-DSC presented in both Figs. 5 and 6, which show that absorbance increases linearly with concentration, and that for concentrations above 6.8×10^{-7} g_{Au}/g_{PEGDA}, less than 4% of the energy from the beam passes through the bulk of the samples.

3.1.3. SPR absorption characterization

Spectrophotometry was used to measure the optical properties of the composite materials both before and after crosslinking. As discussed above, it was found that a peak in SPR absorption exists around 530 nm for both Au colloid solutions and crosslinked com-

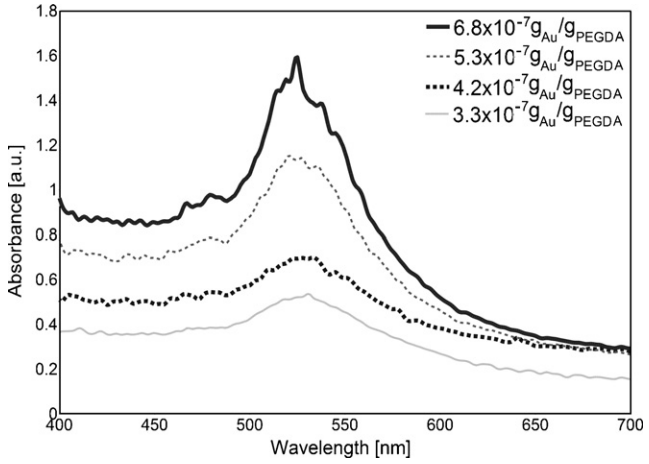

Fig. 5. UV–Vis absorbance spectra of Au/PEGDA composites over a range of nanoparticle concentrations.

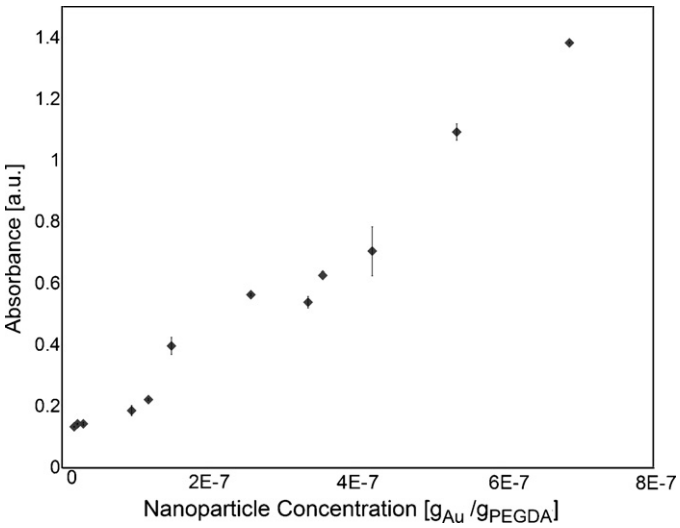

Fig. 6. Magnitude of UV–Vis absorbance at optical excitation wavelength (532 nm) as a function of nanoparticle concentration.

posite materials. It was further found that the magnitude of the absorbance peak increased linearly with concentration, as is shown in Fig. 6 (as expected since more concentrated samples appear darker in color, as can be seen in Fig. 1a).

The SPR resonance peak of the Au nanoparticles was observed to broaden in a composite as compared with the colloidal solution, in a manner consistent with previous theoretical studies of nanoparticle/composite systems [39,40]. Nanoparticles embedded in polymer matrices exhibit peak broadening due to interactions between the nanoparticles and their surroundings, which can include the matrix itself as well as other nearby nanoparticles. A matrix material is able to influence the behavior of embedded particles through its dielectric properties. Plasmon oscillations are electromagnetic in nature, and as such, the local dielectric environment can alter the degree to which oscillations are able to propagate through the matrix and interact with other plasmon absorption centers. As the overall SPR response of a nanocomposite material is related to the sum of the responses from each individual nanoparticle, variations in the local environment of the particles (resulting from both non-uniformities in matrix composition and interparticle spacing) can affect the magnitude, peak position and spectral shape of optical absorbance. These effects can also be altered by the concentration and structure of particles within a matrix. Concentration dependent effects are detailed in the work of Sancho-Parramon [40], which suggests that peak width (measured by FWHM) should increase with increasing particle concentration for an idealized nanoparticle/matrix system. This trend was observed in our work, as shown in Fig. 5, where peak width monotonically increases with increasing nanoparticle concentration. This broadening behavior does not dramatically affect the results in this experiment, as the laser source operates over a sufficiently narrow bandwidth that only absorbance properties at the emission wavelength (532 nm) are of any effect.

3.2. Energy transduction efficiency

An experimental treatment of SPR energy absorption for aqueous suspensions of gold nanoparticles was undertaken by Roper et al. [33], who found that the maximum quantity of heat transferable through optical excitation was given by

$$Q_{max} = I(1 - 10^{-A})\eta_T + Q_0 \quad (1)$$

in which I is the intensity of the incident radiation, A is the absorbance, η_T is the transduction efficiency of the nanoparticle suspension, and Q_0 is the baseline heat flux in the solution measured without nanoparticles. By using a known wavelength of optical radiation and measuring the absorbance of the sample, Eq. (1) can be used to determine the efficiency of heat transfer by analyzing the amount of heat transduced by the particles.

Using Eq. (1) in combination with the measured photo-DSC heating curves and the measured optical absorbance curves, it is possible to calculate the efficiency of energy transduction (η_T) for the polymer/nanoparticle composite materials. In our calculations, we assumed that 4% of the intensity of the input beam would be lost at each interface between the light source and the bulk of the sample due to reflection. This loss can be calculated from the Fresnel equation [41], given that the refractive index of both quartz and crosslinked PEG are approximately equal to 1.5 [42]. The intensity of the light incident on the sample was therefore calculated to be only 88% of the total energy of the laser. In samples of lower concentration, further losses would result as the beam passes out of the sample and is reflected from the bottom of the aluminum pan. These losses were not taken into account in our calculations, since the most concentrated samples should absorb all of the energy from the beam before it reaches the pan. Calculating energy transduction efficiency from all of the samples leads to an average value of $0.82 \pm .1$ as compared to a transduction efficiency of 0.14 ± 0.1 for pure PEGDA. These efficiencies fall between those presented in Roper et al. [33] and Richardson et al. [34], respectively $\eta_T < 0.1$ and $0.97 < \eta_T < 1.03$, for aqueous Au nanoparticle suspensions. The large difference in transduction efficiency measured in this study and that of Roper et al. [33] may be due to the lower excitation wavelength (514 nm) used previously. As in this present investigation, Richardson et al. [34] used an excitation wavelength of 532 nm and their higher measured efficiency may suggest that PEGDA is a less effective host medium for SPR effects than water. Further studies could investigate transduction efficiencies in other host materials to better understand these variations. In addition, some small losses may be due to heat flow to the surroundings due to imperfect insulation in our modified DSC.

3.3. Variations in sample processing parameters

It was found that by varying the processing parameters used to fabricate the composite materials, differences in particle dispersion state could be achieved. Modifying the dispersion properties of the composites was found to affect both the thermal and optical properties of these systems. In particular, the stability of the Au nanoparticles in the uncrosslinked PEGDA solution was found to be highly dependent upon the degree of residual water present after centrifugation and resuspension; at water to monomer ratios of lower than $\sim 0.3\,mL_{H20}/mL_{PEGDA}$, particles were observed to agglomerate, and this was visually apparent as the nanoparticle suspension shifted in color toward a blue/purple. After agglomeration, particles could be separated from the uncrosslinked PEGDA and would retain their altered size upon re-suspension in PEGDA. The time dependence of the agglomeration process was investigated, and absorbance curves taken over time for an uncured composite solution with a water:PEGDA ratio of 0.18 are shown in Fig. 7. Note that the curve at $t = 0$ was taken immediately after the particles were added to the monomer solution. These curves show that when nanoparticles are suspended in a solution of PEGDA with a water:monomer ratio of 0.18, the optical properties change in time. The SPR absorption peak becomes increasingly broad (leading to less selective energy transduction as previously discussed), and the maximum absorbance is shifted to longer wavelengths. This optical broadening occurs as the nanoparticles form clusters of increasing size, altering the electrical properties of the particles, as is described in Link et al. [29].

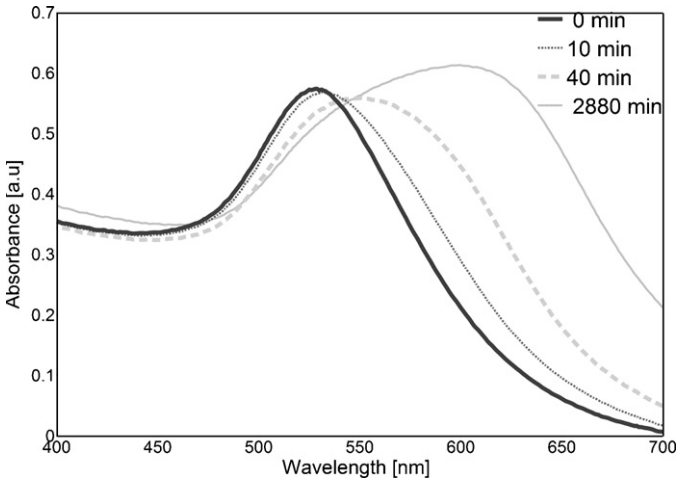

Fig. 7. UV–Vis absorbance spectra for uncured an Au/PEGDA composite solution of 9.8×10^{-8} [g_{Au}/g_{PEGDA}] measured at increasing time intervals after mixing.

Photo-DSC analysis was carried out on composites containing agglomerated nanoparticles, as described previously. At low nanoparticle concentrations, samples with agglomerated nanoparticles transduced energy from the laser source less efficiently, generating ~0.15 W/g less heat flow than well-dispersed samples of the same concentration. As found for well-dispersed samples, with increasing nanoparticle concentration, the magnitude of energy transduced converged to a constant value. Decreased energy transduction can be related to Eq. (1), since as the absorbance of the samples with agglomerated nanoparticles is decreased relative to the well-dispersed composites, the amount of energy which can be extracted from a 532 nm source is decreased. This leads to less effective heating at lower nanoparticle concentrations, although for very high concentrations all of the light is absorbed for both dispersions.

Composites containing poorly dispersed nanoparticle clusters were found to have a transduction efficiency of only 0.48 ± 0.1, further suggesting that higher levels of dispersion lead to more effective heating. These measurements suggest that good particle dispersion is necessary to achieve high energy transduction efficiency, and that care should be taken to prepare composites to ensure that adequate dispersion is maintained.

4. Conclusions

In this investigation, a photo-DSC apparatus was used to characterize the degree of energy transduction in Au/PEGDA nanocomposites when illuminated using a 4.1 mW laser at 532 nm. It was found that high rates of heat flux (up to $0.14\,W/g_{composite}$) could be obtained for relatively low nanoparticle concentrations ($5 \times 10^{-7}\ g_{Au}/g_{PEGDA}$). The rate of heat flux was correlated to both particle concentration and dispersion through measurements of optical absorbance and TEM analysis. The degree of energy transduction measured in this experiment could be easily increased by using a more powerful optical source, of which both a laser or narrow band LED would be sufficient to maintain selective heating; as such, the magnitude of heating could be altered to suit a variety of applications such as remotely powered microfluidic heaters. Photo-DSC was demonstrated as a method to characterize heat flow in the nanocomposite systems and was shown to be both reliable and precise. The efficiency of energy transduction in our composite system was 0.82 ± 0.1. It was also found that improved nanoparticle dispersion leads to more effective energy transduction. The information presented in this study lays the groundwork for future investigations of the mechanisms of energy transfer in noble metal nanocomposites, as well as for studying the properties of gold nanoparticles employed in the treatment of cancer by hyperthermia. Our results will also be beneficial for optimizing the properties of functional stimulus-responsive materials based upon Au/PEGDA composite materials, for use in systems where remote actuation is an advantage, including drug delivery vehicles and microfluidic devices.

Acknowledgements

The authors would like to thank Brian Worfolk for assistance with TEM characterization, Andrew Bonifas for assistance with laser intensity measurements, as well as Y. Maham for helpful discussion. Funding from the MicroSystems Technology Research Initiative (MSTRI) and the Natural Sciences and Engineering Research Council of Canada (NSERC) is gratefully acknowledged. Access to the DSC was provided by the Integrated Nanosystems Research Facility (INRF) and the National Institute for Nanotechnology. B.N. would like to thank Alberta Ingenuity, now a part of Alberta Innovates – Technology Futures, for financial support.

References

[1] R. Mohr, K. Kratz, T. Weigel, M. Lucka-Gabor, M. Moneke, A. Lendlein, Initiation of shape-memory effect by inductive heating of magnetic nanoparticles in thermoplastic polymers, PNAS 103 (2006) 3540–3545.
[2] A.J. Ryan, C.J. Crook, J.R. Howse, P. Topham, M. Geoghegan, S.J. Martin, A.J. Parnell, L. Ruiz-Perez, R.A. Jones, Mechanical actuation by responsive polyelectrolyte brushes and triblock gels, J. Macromol. Sci. Part B Phys. 44 (2005) 1103–1121.
[3] A. Suzuki, T. Ishii, Y. Maruyama, Optical switching in polymer gels, J. Appl. Phys. 80 (1996) 131–136.
[4] J.F. Mano, Stimuli-responsive polymeric systems for biomedical applications, Adv. Eng. Mater. 10 (2008) 515–527.
[5] Y. Osada, H. Okuzaki, H. Hori, A polymer gel with electrically driven motility, Nature 355 (1992) 242–244.
[6] T.Y. Liu, K.H. Liu, D.M. Liu, S.Y. Chen, I.W. Chen, Temperature-sensitive nanocapsules for controlled drug release caused by magnetically triggered structural disruption, Adv. Funct. Mater. 19 (2009) 616–623.
[7] S.H. Hu, S.Y. Chen, D.M. Liu, C.S. Hsiao, Core/single-crystal-shell nanospheres for controlled drug release via a magnetically triggered rupturing mechanism, Adv. Mater. 20 (2008) 2690–2695.
[8] V.M. De Paoli, L.S.H. De Paoli, L. Spinu, B. Ingber, Z. Rosenzweig, N. Rosenzweig, Effect of oscillating magnetic fields on the release properties of magnetic collagen gels, Langmuir 22 (2006) 5894–5899.
[9] V. Cauda, C. Argyo, A. Schlossbauer, T. Bein, Controlling the delivery kinetics from colloidal mesoporus silica nanoparticles with pH-sensitive gates, J. Mater. Chem. 20 (2010) 4305–4311.
[10] S.K. Baek, J. Min, J.H. Park, Wireless induction heating in a microfluidic device for cell lysis, Lab Chip 10 (2010) 909–917.
[11] S. Ghosh, C. Yang, T. Cai, Z. Hu, A. Neogi, Oscillating magnetic field-actuated microvalves for micro- and nanofluidics, J. Phys. D: Appl. Phys. 42 (2009) 135501.
[12] J.Y. Park, P. Daksha, G.H. Lee, S. Woo, Y. Chang, High water-dispersible PEG surface modified ultra small superparamagnetic iron oxide nanoparticles useful for target-specific biomedical applications, Nanotechnology 19 (2008) 365603.
[13] A.S. Eggeman, S.A. Majetich, D. Farrell, Size and concentration effects on high frequency hysteresis of iron oxide nanoparticles, IEEE Trans. Electromagn. 43 (2007) 2451–2453.
[14] C.M. Yakacki, N.S. Satarkar, K. Gall, R. Likos, J.Z. Hilt, Shape-memory polymer networks with Fe_3O_4 nanoparticles for remote actuation, J. Appl. Polym. Sci. 112 (2009) 3166–3176.
[15] A. Henglein, Small-particle research: physiochemical properties of extremely small colloidal metal and semiconductor particles, Chem. Rev. 89 (1989) 1861–1873.
[16] K.H. Su, Q.H. Wei, X. Zhang, Interparticle coupling effects on plasmon resonances of nanogold particles, Nano Lett. 3 (2003) 1087–1090.
[17] K.L. Kelly, The optical properties of metal nanoparticles: the influence of size, shape, and dielectric environment, J. Phys. Chem. B 107 (2003) 668–677.
[18] E. Hutter, J.H. Fendler, Exploitation of localized surface plasmon resonance, Adv. Mater. 16 (2004) 1685–1706.
[19] S. Bruzzone, M. Malvaldi, Local field effects on laser-induced heating of metal nanoparticles, J. Phys. Chem. C 113 (2009) 15805–18510.
[20] E. Dulkeith, T. Niedereichholz, T.A. Klar, J. Feldmann, G. von Plessen, D.I. Gittins, K.S. Mayya, F. Caruso, Plasmon emission in photoexcited, gold nanoparticles, Phys. Rev. B 70 (2004) 205424.
[21] D.L. Zhao, X.X. Wang, X.W. Zeng, Q.S. Xia, J.T. Tang, Preparation and inductive heating property of Fe_3O_4-chitosan composite nanoparticles in an AC magnetic field for localized hyperthermia, J. Alloys Compd. 477 (2009) 739–743.

[22] X. Huang, P.K. Jain, I.H. El-Sayed, M.A. El-Sayed, Determination of the minimum temperature required for selective photothermal destruction of cancer cells with the use of immunotargeted gold nanoparticles, Photochem. Photobiol. 82 (2006) 412–417.
[23] R.K. Visaria, R.J. Griffin, B.W. Williams, E.S. Ebbini, G.F. Paciotti, C.W. Song, J.C. Bischof, Enhancement of tumor thermal therapy using gold nanoparticle-assisted tumor necrosis factor-A delivery, Mol. Cancer Ther. 5 (2006) 1014–1020.
[24] I.H. El-Sayed, X. Huang, M.A. El-Sayed, Selective laser photo-thermal therapy of epithelial carcinoma using anti-EGFR antibody conjugated gold nanoparticles, Cancer Lett. 239 (2006) 129–135.
[25] J.J. Mock, M. Barbic, D.R. Smith, D.A. Schultz, S. Schultz, Shape effects in plasmon resonance of individual colloidal silver nanoparticles, J. Chem. Phys. 116 (2002) 6755–6759.
[26] J. Homola, Present and future of surface plasmon resonance biosensors, Anal. Bioanal. Chem. 377 (2003) 528–539.
[27] A.D. McFarland, R.P. Van Duyne, Single silver nanoparticles as real-time optical sensors with zeptomole sensitivity, Nano Lett. 3 (2003) 1057–1062.
[28] K.S. Lee, M. El-Sayed, Gold, Silver nanoparticles in sensing and imaging: sensitivity of plasmon response to size, shape, and metal composition, J. Phys. Chem. B 110 (2006) 19220–19225.
[29] S. Link, M.A. El-Sayed, Shape and size dependence of radiative, non-radiative and photothermal properties of gold nanoparticles, Int. Rev. Phys.Chem. 19 (2000) 409–453.
[30] I.L. Maksimova, G.G. Akchurin, B.N. Khlebtsov, G.S. Terenyuk, I.A. Ermolaev, A.A. Skaptsov, E.P. Soboleva, N.G. Khlebtsov, V.V. Tuchin, Near-infrared laser photothermal therapy of cancer by using gold nanoparticles: computer simulations and experiment, Med. Laser Appl. 22 (2007) 199–206.
[31] H.H. Richardson, A.C. Thomas, M.T. Carlson, M.E. Kordesch, A.O. Govorov, Thermo-optical response of nanoparticles: melting of ice and nanocalorimetry approach, J. Electron. Mater. 36 (2007) 1587–1593.
[32] M.B. Cortie, N. Harris, M.J. Ford, Plasmonic heating and its possible exploitation in nanolithography, Physica B 394 (2007) 188–192.
[33] D.K. Roper, W. Ahn, M. Hoepfner, Microscale heat transfer transduced by surface plasmon resonant gold nanoparticles, J. Phys. Chem. C 111 (2007) 3636–3641.
[34] H.H. Richardson, M.T. Carlson, P.J. Tandler, P. Hernandez, A.O. Govorov, Experimental, theoretical studies of light-to-heat conversion and collective heating effects in metal nanoparticle solutions, Nano Lett. 9 (2009) 1139–1146.
[35] M.J.M. Abadie, Y. Xiong, F.Y.C. Boey, UV photo curing of N,N-bismaleimido-4-4-diphenylmethane, Eur. Polym. J. 39 (2003) 1243–1247.
[36] W.S. Kim, K.S. Park, J.H. Nam, D. Shin, S. Jang, T.Y. Chung, Fast cure kinetics of a UV-curable resin for UV nano-imprint lithography: phenomenological model determination based on differential photocalorimetry results, Thermochim. Acta 498 (2010) 117–123.
[37] V.V. Yu, N.F. Lin, K.C. Ling, A. Marc, Kinetic analysis of UV-curable epoxy resins for micromachining applications, Adv. Mater. Res. 74 (2009) 299–302.
[38] H. Fischer, R. Baer, R. Hany, I. Verhoolen, M. Walbiner, 2,2-Dimethoxy-2-phenylcacetophenone: photochemistry and free radical fragmentation, J. Chem. Soc. Perkin Trans. 2 (1990) 787–798.
[39] J. Zhu, Local environment dependant line width of plasmon absorption in gold nanoshell: effects of local filed polarization, Appl. Phys. Lett. 92 (2008) 241919.
[40] J. Sancho-Parramon, Surface plasmon resonance based broadening of metallic particles in the quasi-static approximation: a numerical study of size confinement and interparticle interaction effects, Nanotechnology 20 (2009) 235706.
[41] M. Born, E. Wolf, Principles of Optics, seventh ed., Cambridge University Press, Cambridge, 1999.
[42] W.C. Chen, C.C. Chang, Synthesis and characterization of large diameter acrylic polymer light conduits, J. Mater. Chem. 9 (1999) 2307–2312.